Branching ratios in the radiative decay of helium doubly excited states

M. Coreno,[1,3,*] K. C. Prince,[2,3] R. Richter,[2] M. de Simone,[3] K. Bučar,[4] and M. Žitnik[4]
[1]*CNR-IMIP, Area della Ricerca di Roma 1, Montelibretti (Rome), I-00016 Italy*
[2]*Sincrotrone Trieste, in Area Science Park, I-34012 Basovizza (Trieste), Italy*
[3]*CNR-Laboratori TASC-INFM, in Area Science Park, Loc. Basovizza, I-34012 Trieste, Italy*
[4]*J. Stefan Institute, 1000 Ljubljana, Slovenia*
(Received 15 September 2004; published 23 November 2005)

The doubly excited singlet states of He below the $N=2$ threshold may decay by autoionization or fluorescence. In the fluorescence decay channel, most decay cascades consist of emission of three photons, of which the first is a VUV photon, the second is in or near the visible range, and the last is another VUV photon. We have studied the fluorescence channel decay dynamics of the $(2,0_n)$, $(2,1_n)$ and $(2,-1_n)$ ^{1}P, $n=3-7$, states by wavelength dispersed photon-induced fluorescence spectroscopy. We have detected the photons in the second step of the cascade and determined the branching ratios for the strongest lines in this step. From these data we are able to calculate the branching ratios of the first step in the cascade. The results are in good agreement with calculations of the main decay channels of the higher resonances, but about 20–30 % lower, and so we are able to describe quantitatively the whole fluorescence cascade of the above-mentioned doubly excited states.

DOI: 10.1103/PhysRevA.72.052512 PACS number(s): 32.70.Cs, 32.50.+d

I. INTRODUCTION

The doubly excited states of He constitute a prototype quantum three-body system, and attempts were made to observe them as early as 1930 [1]. After Madden and Codling reported the discovery of the strongest optically allowed states below $N=2$ [2] there was relatively little experimental progress until Domke *et al.* [3] undertook high resolution studies of ion yield spectra of the three theoretically predicted singlet series converging to the $N=2$ threshold, as well as higher series. In the 1990s, our understanding of He and its interaction with radiation advanced rapidly with new experimental methods, such as total UV fluorescence and metastable atom yield spectroscopy [4–6]. It was concluded that the cross section is strongly influenced by the fluorescence decay channel [5] and this was later verified by comparing ion yield spectra and absolute cross section [7], where strong differences were observed. More recently a careful photoemission study has provided evidence of nondipole transitions [8] in the absorption spectrum of He. To date all of the theoretically predicted singlet series converging to the $N=2$ threshold, and members of three triplet series, $(2,0_n)$ ^{3}D^o and $(2,0_n)$, $(2,-1_n)$ ^{3}P^o, have been observed [9–11]. (The notation is that used by Domke *et al.* [3])

Although our understanding of the cascade processes occurring on deexcitation of the doubly excited helium atom is increasing, there has been only one observation of the branching ratios of the decay channels by Schartner *et al.* [12]. They published VUV fluorescence spectra of emission from the singlet states and relative intensities of some of the near visible emission lines. They showed that the main decay channels observed by photon-induced fluorescence spectroscopy (PIFS) for the $(2,-1_4)$ and $(2,-1_6)$ states were via the $1s4d-1s2p$ to $1s6d-1s2p$ channels, respectively, while the $(2,0_n)$ and $(2,1_n)$ states decayed via both $1sns$ and $1snd$ transitions to $1s2p$.

In the present work we have measured the PIFS of helium in the double excitation region below the $N=2$ threshold and extended this work. We present PIFS results concentrating on the lower resonances, particularly the nearby groups of $(2,-1_{n-1})$, $(2,1_n)$ and $(2,0_n)$ ^{1}P states, for $n=3-7$. Apart from the work of Schartner *et al.*, very little is known about the fluorescence decay dynamics of these states. The conventional approach would be to measure the energy resolved VUV spectrum, but the restricted angular acceptance of grating spectrometers, and limited intensity of grazing incidence instruments means that this experiment is rather difficult. By concentrating on the second decay step, involving visible light, we are able to use a spectrometer with high luminosity and resolution. Efficiency is maintained because the quantum yields of VUV and visible photons are similar. Thus the present approach allows us to obtain detailed information about the decay dynamics in an experimentally more efficient mode.

II. EXPERIMENTAL

The measurements were carried out at the gas phase photoemission beamline [13], Elettra synchrotron radiation laboratory, Trieste. A photon bandwidth of 2 meV was used in the excitation of higher resonances and of 4 meV for the lower, broader resonances. The PIFS setup, available at the Gas Phase beamline, is the object of a separate publication [14] and it is outlined briefly here. It consists of two independently pumped vacuum chambers, one behind the other, of which the first is devoted to the dispersed fluorescence experiment. A gas cell for ion yield and absolute photoabsorption measurements is placed in a series behind the first chamber, at the end of the beamline [7]. For nondispersed

*Author to whom correspondence should be addressed. Email: marcello.coreno@elettra.trieste.it

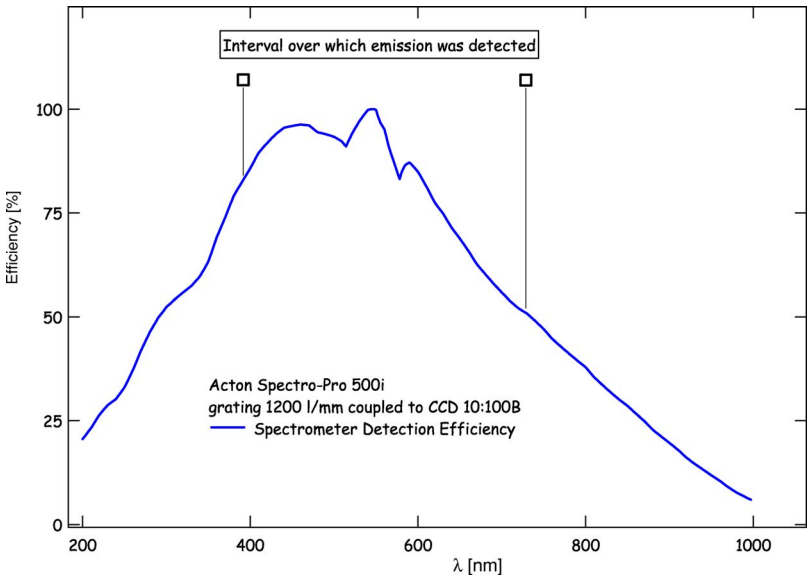

FIG. 1. (Color online) Plot of the detection efficiency of the fluorescence spectrometer calculated from the manufacturer's data. It results from the product of the Acton 500I spectrometer transmission and the CCD quantum efficiency.

VUV fluorescence yield, a detector based on a YAP (yttrium aluminum perovskite) scintillator crystal has been inserted in the gas cell. With this experimental setup it is possible to measure simultaneously all three spectra: PIFS, ion yield, and VUV fluorescence yield.

The chamber for dispersed fluorescence is pumped by a 1000 l/sec turbo pump and gas is introduced into the chamber via a hypodermic needle. Light is collected along the (horizontal) electric vector of the linearly polarized incident synchrotron radiation. The fluorescence spectrometer is an Acton 500i monochromator, coupled to a Princeton model 10:100B CCD detector, operated at a temperature of 163 K. The spectrometer resolution was typically set to 1 nm (0.25 nm for some high resolution measurements) which is adequate to resolve lines in the He I series which were relevant to this study.

The detection efficiency of our spectrometer was calculated on the basis of the manufacturer's data and is shown in Fig. 1. Detection efficiency was also checked in the 350–750 nm wavelength region by an independent measurement with a calibrated tungsten halogen lamp [Ocean Optics, model HL-2000]. Our independent calibration of the relative transmission agrees with the curve within 8%. In this way we also obtained an estimate for the error of ±4% in the relative intensity of the observed lines. Unfortunately in our present experiment the error in the relative intensity for emission lines recorded in different CCD windows and/or from the decay of different excited states may be higher due to the drift of the incident light photon energy. The resonances are very narrow, and small shifts (due to thermal drift of the monochromator mechanics, beam movement, etc.) caused significant changes in the VUV partial fluorescence yield. For this reason, the spectra from different resonances were not normalized to one another. Instead the PIFS intensity at each resonance is normalized to unity for the maximum of the strongest peak. For the lower resonances, where the emission occurs at widely different wavelengths, we present only qualitative data. For the higher resonances, the main emission lines occur close together and are acquired in a single window by the CCD. This means that relative intensities are not affected by factors such as photon energy drift, pressure variations, or beam movements, and we expect much better accuracy. We have therefore concentrated on these data.

We checked for pressure effects by scanning wide ranges of emission wavelength. At high pressure, a number of unexpected lines were observed and the most significant emission was observed for the triplet ($1s3d \rightarrow 1s2p$, ^{3}D-^{3}P) and ($1s3s \rightarrow 1s2p$, ^{3}S-^{3}P) transitions, as well as the singlet transition ($1s3p \rightarrow 1s2s$, ^{1}P-^{1}S) which is otherwise expected to be generally weak (it can occur via cascade processes). To optimize the pressure, the incident photon energy was set to a resonance giving rise to emission near this last transition wavelength of 501.7 nm, such as the $(2,1_5)$ resonance. The local pressure was then changed by moving the needle or adjusting the gas inlet valve while observing the intensity ratio of the expected lines to that of the 501.7 nm line. When the intensity of this line was below about 2% of the nearby allowed $1s4d \rightarrow 1s2p$ transition at 492.2 nm, no other spurious lines were present in the spectrum. This extraneous emission is believed to be due to the collision of photoelectrons with neutral ground state helium atoms, so for higher resonances the problem is the same or reduced, as the photoionization cross section is similar or decreases. For this reason the pressure was optimized on lower resonances and left constant at higher resonances, where the emission was weaker and therefore more difficult to detect. Typical chamber pressure was 2×10^{-5} mbar, but the local pressure near the needle was estimated to be higher by one to two orders of magnitude.

An example of a partial VUV fluorescence spectrum taken simultaneously with an ion yield spectrum is shown in Fig. 2. As expected fluorescence yield consists of Lorentzian peaks [5,10], whose intensity is not directly related to the ion yield intensity. This peak shape facilitates the location of the singlet doubly excited states, particularly for the $(2,-1_n)$ and $(2,1_n)$ series which become quite weak in ion yield spectra for higher values of n. This is relevant to the $(2,-1_{n-1})$ and $(2,1_n)$ pairs of states which are close together energetically, where the Fano profile of the latter state in ion yield spectra hampers resolution of these states.

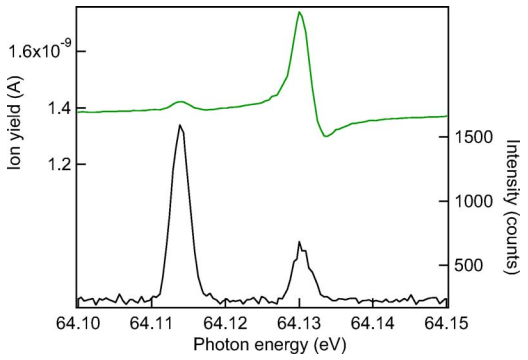

FIG. 2. (Color online) Ion yield (upper curve, left scale) and fluorescent UV photon yield (lower curve, right scale) at the $(2,-1_3)$, $(2,1_4)$ resonances.

Incident photon energies were calibrated to the values given in [3], and fluorescent photon wavelengths were calibrated to the values in the NIST database [15].

III. CALCULATIONS

The wave functions of $J=1$ doubly excited states, accessible by one photon absorption from the ground state of helium, were obtained by truncated diagonalization of the nonrelativistic Hamiltonian [16]. The lowest 44 discrete eigenstates with either ^{1}P, ^{3}P, or ^{3}D odd symmetry above the first ionization threshold were calculated. The states were expanded in the basis set of two-electron configurations $\alpha_a = nln'(l+1)$ of matching symmetry,

$$|iLS\rangle = \sum_a c_{ia}|\alpha_a LS\rangle$$

with n, n' ranging from 2 to 12 and l from 0 to 3 [17]. Once the resonance is created it may release its energy by a fluorescence transition into one of the four series of states converging to the first ionization threshold, as exemplified in Fig. 3. Due to the dipole selection rules, the following singly excited states are populated:

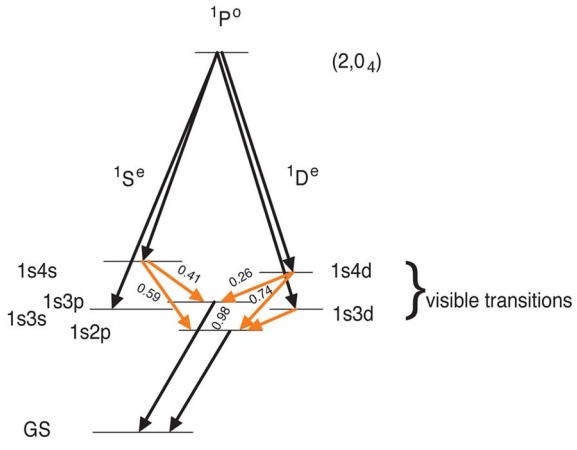

FIG. 3. (Color online) Cascade processes for the ^{1}P^o $(2,0_4)$ state to singlet states. The angled numbers on the arrows indicate branching ratios. Where no numbers are indicated for visible wavelength transitions, the branching ratio is 1. For the upper, VUV transitions, the branching ratio is to be determined. GS indicates ground state.

$$^1\mathrm{P}_1^0 \rightarrow 1sns(^1\mathrm{S}_0^e), 1snd(^1\mathrm{D}_2^e),$$

$$^3\mathrm{P}_1^0 \rightarrow 1sns(^3\mathrm{S}_0^e), 1snd(^3\mathrm{D}_{1,2}^e),$$

$$^3\mathrm{D}_1^0 \rightarrow 1snd(^3\mathrm{D}_{1,2}^e).$$

These states were calculated one by one up to $n=8$ by minimizing the energy of the corresponding reduced pair configuration expansion in the MCHF (multi configuration Hartree Fock) approximation [18]:

$$|jL'S\rangle = \sum_b c_{jb}|\alpha_{jb}L'S\rangle.$$

The partial fluorescence rate $\Gamma_{j,i}^r$ of the ith resonance ending in the jth state is obtained by multiplying $(\frac{4}{3})\ \alpha^3\ (\mathrm{E_i}\text{-}\mathrm{E_j})^3$ by

$$\tfrac{1}{3}\mathrm{S_{ji}}(^1\mathrm{P} \rightarrow {}^1\mathrm{S}), \quad \tfrac{1}{3}\mathrm{S_{ji}}(^1\mathrm{P} \rightarrow {}^1\mathrm{D}), \quad \tfrac{1}{3}\mathrm{S_{ji}}(^3\mathrm{P} \rightarrow {}^3\mathrm{S}),$$

$$\tfrac{1}{3}\mathrm{S_{ji}}(^3\mathrm{P} \rightarrow {}^3\mathrm{D}) + \tfrac{1}{5}\mathrm{S_{ji}}(^3\mathrm{D} \rightarrow {}^3\mathrm{D})$$

for $1sns(^1\mathrm{S})$, $1snd(^1\mathrm{D})$, $1sns(^3\mathrm{S})$, and $1snd(^3\mathrm{D})$ states, respectively. The line strengths above are defined by

$$\mathrm{S_{ji}}(\mathrm{LS} \rightarrow \mathrm{L'S}) = \left| \sum_{b,a} c_{jb}c_{ia}\langle \alpha_{jb}\mathrm{L'S}\|\mathrm{E}^1\langle \alpha_{ai}\mathrm{LS}\rangle \right|^2,$$

where

$$\mathrm{E_m^1} = \sqrt{\frac{4\pi}{3}}[r_1 Y_{1m}(\hat{1}) + r_2 Y_{1m}(\hat{2})]$$

is the electric dipole tensor operator for the helium atom. The states created by primary fluorescence may decay further in a relatively fast process by secondary photon emission ending up in the allowed singly excited states of lower energy,

$$1sns(^{1,3}\mathrm{S}) \rightarrow 1smp(^{1,3}\mathrm{P}),$$

$$1snd(^{1,3}\mathrm{D}) \rightarrow 1smp(^{1,3}\mathrm{P}), 1smf(^{1,3}\mathrm{F}).$$

These newly populated states are not in the ground state and release their excess energy by fluorescence. In order to follow the cascade we have calculated the dipole transition rates connecting pairs of $1snl$ states within the $n \leqslant 8$, $l \leqslant 3$ set. A comparison of our *ab initio* calculated fluorescence rates [17] to the previously published semiempirical set of values [19] shows that the agreement is always better than 1%.

In order to estimate the relative fluorescence yields emitted in the visible part of the spectrum we have combined partial fluorescence decay rates $\Gamma_{j,i}^r$ of the ith doubly excited state, calculated in the length and velocity form, with the previously published extended list of branching ratios connecting singly excited states in helium [19]. The occurrence of 36 $k \rightarrow k'$ transitions in the visible

$$\begin{array}{ll} \text{singlet:} & \text{triplet:} \\ 1sns \rightarrow 1s2p(k=1-6,k'=1), & 1sns \rightarrow 1s2p(k=19-24,k'=3), \\ 1snp \rightarrow 1s2s(k=7-12,k'=2), & 1snp \rightarrow 1s2s(k=25-30,k'=4), \\ 1snd \rightarrow 1s2p(k=13-18,k'=1), & 1snd \rightarrow 1s2p(k=31-36,k'=3), \end{array} \tag{1}$$

with n running from 3–8 was followed separately step by step in the cascade decay to accumulate the corresponding fluorescence yields. The wavelengths of these transitions fit the detector window and their intensity is expected to be different from zero as they are found on the decay path of the resonances. Since we measure steady state fluorescence yields and not their time dependence, it is enough to calculate the cascade process until equilibrium is reached (all atoms in ground or metastable states,) and compare this with the measurement. The yield $I_{kk'}$ is then obtained by summing up for each step of the cascade the occupation A_{nk}, transferred to the kth state from all higher lying singly excited states in the previous cascade step, weighted by the branching ratio $B_{k,k'}$ for the $k \rightarrow k'$ transition:

$$I_{\mathrm{k,k'}} = B_{k,k'} \sum_{n=1}^{N} A_{n,k}. \tag{2}$$

The initial occupation $A_{1,p}$ of singly excited states occurs at time zero due to the primary fluorescence decay of the parent ith resonance:

$$A_{1,p} = \frac{\Gamma^{\mathrm{r}}_{\mathrm{p,i}}}{\sum_p \Gamma^{\mathrm{r}}_{\mathrm{p,i}}}$$

when only $A_{1,j} \neq 0$. The occupation of the pth state is propagated along the cascade by summing up the occupations of higher lying $q > p$ states weighted with the corresponding decay branching ratios $B_{q,p}$:

$$A_{n,p} = \sum_{q>p} A_{n-1,q} B_{q,p}.$$

The fluorescence yields (2) converge very fast. The series can be typically truncated at $n=7$, and for the transitions under study, terms $A_{\mathrm{n>1,k}}$ represent only a small correction to the leading term $A_{\mathrm{1,k}}$.

The calculations show small differences between the length and velocity form distribution of fluorescence yields. The maximum difference occurs for the 2+ state, where differences of up to 15% are present, but experimentally the fluorescence from this state was too weak to measure (the state decays mostly by autoionization). For $n > 4$, the differences are of the order 1% and we have used the calculated values for the length form.

Transitions from the doubly excited singlet states to intermediate triplet states are predicted to be weak [17] and experimentally we did not observe any triplet-triplet transitions for singlet state excitation. On excitation of the recently observed [10] triplet 7^{3D} and 8^{3D} states (notation of Penent *et al.*, Ref. [10]), weak fluorescence was observed at 370.8 nm ($1s7d-1s2p$, ^{3}P-^{3}D) and 363.4 nm ($1s8d-1s2p$, ^{3}P-^{3}D), respectively [14]. Triplet emission is still under study, but otherwise we do not report any other results here.

Finally, the emission anisotropy has also been taken into account for the experimental arrangement used. The β parameter for emission from $1sns$ states in the second step of the cascade decay of the resonance is zero (isotropic emission) while that for $1snd$ states is $-\frac{7}{20}$ [17]. For the comparison with the measured data all the calculated $1snd \rightarrow 1s2p$ yields (2) were multiplied by a factor $Y=0.66$ to take account of this anisotropy and the finite acceptance angle of the detector.

IV. RESULTS

No visible fluorescence was detected at the $(2,0_2)$ resonance. The state decays mostly by autoionization, and so the fluorescence is expected to be weak.

The first spectra acquired in this experiment were taken over a wide emission energy range, with each spectrum being about 80 nm wide, and overlapping to cover the spectral range from 350 to 750 nm. It was verified that the theory predicted the emission lines rather well and then the emission ranges measured were restricted to the main lines.

Figure 4 shows the PIF spectra of helium at the $(2,0_3)$ and $(2,1_3)$ resonances. For these states, the emission lines are at widely spaced wavelengths and as we do not consider the calculated transmission of the system, Fig. 1, to be suf-

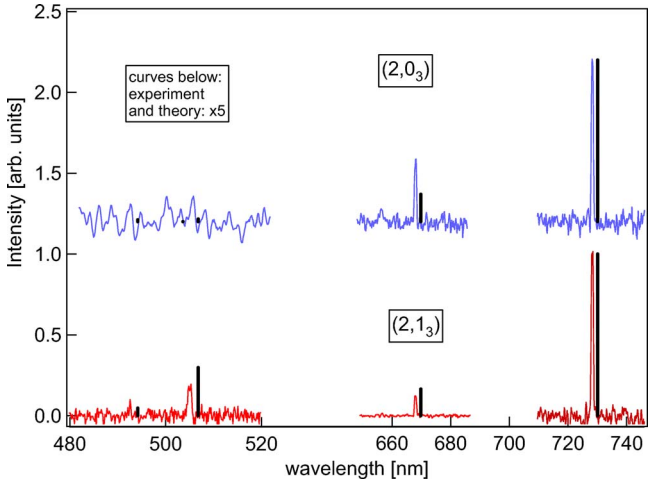

FIG. 4. (Color online) PIF spectra for excitation at the $(2,0_3)$ and $(2,1_3)$ resonances. The black bars to the right of each peak indicate the theoretical intensity, offset 2 nm horizontally for clarity.

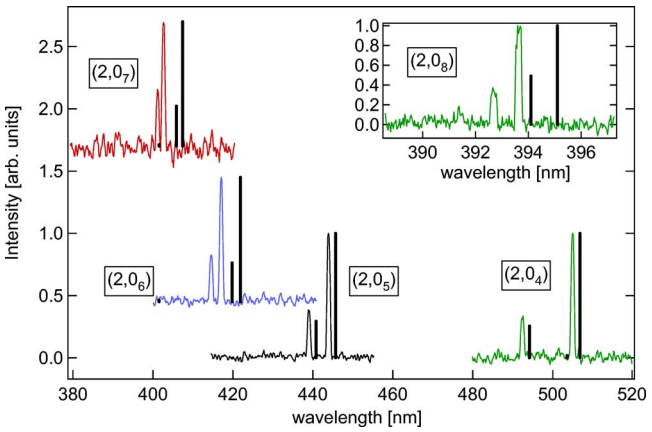

FIG. 5. (Color online) PIF spectra showing the strongest lines for excitation to the $(2,0_n)$ states. Inset: $(2,0_8)$ region taken at resolution 0.25 nm.

ficiently reliable, it is not possible to differentiate discrepancies between theory and experiment from variations of the spectrometer transmission. We note that the theory predicts a roughly equal ratio of intensity for the 728.1 nm ($1s3s \rightarrow 1s2p$) and 667.8 nm ($1s3d \rightarrow 1s2p$) lines, while the experiment shows that for the $(2,1_3)$ state the 667.8 nm line is a little weaker, and for the $(2,0_3)$ state, it is stronger. The theory predicts appreciable intensity at 492.2 nm ($1s4d \rightarrow 1s2p$) and 504.8 nm ($1s4s \rightarrow 1s2p$) for the $(2,1_3)$ state, but not for the $(2,0_3)$ state and this is qualitatively consistent with the observations.

The strongest lines of the $(2,0_n)$, $n=4-8$, emission spectra are shown in Fig. 5. The experimental spectra have been normalized to a value of 1 for the strongest peak, and likewise for the theoretical values, which are shown as bars, slightly displaced from the experimental curve. The spectra consist of two main lines, and for the $(2,0_n)$ state the lines are the $1snd \rightarrow 1s2p$ and $1sns \rightarrow 1s2p$ transitions at shorter and longer wavelength, respectively. The observed lines and their assignments are summarized in Table I, and the relative intensities are summarized in Table II. It can be seen from the data that the agreement is acceptable, with a discrepancy between theory and experiment of about 20%.

Figure 6 shows the second state in the $(2,1_n)$ series, $n=4$. The emission lines are spread over a wide range, and again the calculated transmission of the spectrometer is only a qualitative guide. The theory however correctly predicts the four strongest lines with a relative intensity that is not too far from the experimental value. For a quantitative comparison, we compare the third and fourth strongest lines, which occur in the same wavelength window.

For the $n=5$ to 7 members of the $(2,1_n)$ series, Fig. 7, the four strongest lines occur close together and the transmission of the spectrometer changes only slightly over this narrow range, so that the correction for transmission can introduce only a small error. The strongest doublet of each $(2,1_n)$ resonance is due to the $1s(n-1)d \rightarrow 1s2p$ and $1s(n-1)s \rightarrow 1s2p$ transitions at shorter and longer wavelength, respectively, but note that the relative intensity is reversed with respect to $(2,0_n)$ lines, as the $1s(n-1)s$ transition is much stronger in this case. The weaker pairs of peaks are due to the $1snd \rightarrow 1s2p$ and $1sns \rightarrow 1s2p$ transitions and they have a different intensity ratio. The calculations reproduce well the intensity ratio of the $1sns$ and $1snd$ transitions, and also the relative intensity for the second pair of peaks for the $(2,1_5)$ state. At higher values of n there is a tendency to overestimate the intensity of the ns and nd transitions.

The third series investigated was the $(2,-1_n)$ series, Figs. 8 and 9. The main peaks of the $(2,-1_3)$ state are due to $1s3d \rightarrow 1s2p$, $1s4s \rightarrow 1s2p$ and $1s3s \rightarrow 1s2p$ transitions, in order of predicted and observed intensity. As the peaks are widely spaced, it is not possible to identify discrepancies between theory and experiment, but the results are qualitatively consistent within the expected variation of spectrometer transmission. The $(2,-1_n)$ states $(n=4-7)$ decay almost exclusively to $1snd$ intermediate states, with only weak transitions to $1sns$ states. As a result, it is difficult to quantify the relative branching ratio: the weaker channels can be detected but have low signal-to-noise ratio. Overall the intensity ratio shows the behavior predicted by theory.

TABLE I. Observed wavelengths and their assignments. All transitions are $^1S^e$-$^1P^o$ ($1sns$ upper states) or $^1D^e$-$^1P^o$ ($1snd$ upper states). Wavelengths have been calibrated to the NIST database values [15].

Wavelength (nm)	Assignment	Doubly excited parent states for which emission was observed
392.65	$1s8d-1s2p$	$(2,0_8)$
393.59	$1s8s-1s2p$	$(2,0_8)$
400.92	$1s7d-1s2p$	$(2,0_7),(2,1_7)$
402.40	$1s7s-1s2p$	$(2,0_7),(2,1_7)$
414.37	$1s6d-1s2p$	$(2,0_6),(2,1_6),(2,01_7),(2,-1_6)$
416.90	$1s6s-1s2p$	$(2,0_6),(2,1_6),(2,1_7)$
438.80	$1s5d-1s2p$	$(2,0_5),(2,1_5),(2,1_6),(2,-1_5)$
443.75	$1s5s-1s2p$	$(2,0_5),(2,1_5),(2,1_6)$
492.19	$1s4d-1s2p$	$(2,0_4),(2,1_3),(2,1_4),(2,1_5),(2,-1_4)$
504.77	$1s4s-1s2p$	$(2,0_3),(2,0_4),(2,1_3),(2,1_4),(2,1_5),(2,-1_3),(2,-1_4)$
667.81	$1s3d-1s2p$	$(2,0_3),(2,1_3),(2,1_4),(2,-1_3)$
728.13	$1s3s-1s2p$	$(2,0_3),(2,1_3),(2,1_4),(2,-1_3)$

TABLE II. Experimental and theoretical branching ratios for VUV fluorescent decay from He doubly excited states. Velocity (length) indicates the gauge used for the calculations.

Upper state	Strongest fluorescent decay channels $1sns$, $1snd$	Experimental visible fluorescence branching ratio, $\frac{I(1sns-1s2p)}{I(1snd-1s2p)}$ Estimated error: ±4%.	Derived experimental partial VUV fluorescence branching ratio, $\left(\frac{\Gamma^r_{1sns,i}}{\Gamma^r_{1snd,i}}\right)_{exp}$ ±4%	Theoretical partial branching ratio [17], $\frac{\Gamma^r_{1sns,i}}{\Gamma^r_{1snd,i}}$ Velocity (Length)	Theoretical total branching ratio [17], $\frac{\Gamma^r_{s,i}}{\Gamma^r_{d,i}}$ (velocity)	Schartner *et al.* [12] experiment $\frac{\Gamma^r_{1sns,i}}{\Gamma^r_{1snd,i}}$	Mickat *et al.* [22] experiment $\frac{\Gamma^r_{1sns,i}}{\Gamma^r_{1snd,i}}$	Liu *et al.* [21] theory $\frac{\Gamma^r_{s,i}}{\Gamma^r_{d,i}}$
$(2,0_4)$	$1s4s$, $1s4d$	2.9	2.4	3.22 (3.21)	3.26	5	2.4	2.92
$(2,0_5)$	$1s5s$, $1s5d$	2.7	2.4	3.08 (3.05)	3.08		3.1	2.70
$(2,0_6)$	$1s6s$, $1s6d$	2.6	2.5	3.03 (3.02)	3.03	5	3.4	2.75
$(2,0_7)$	$1s7s$, $1s7d$	2.6	2.5	3.03 (3.03)	3.03		3.6	2.72
$(2,1_4)$	$1s3s$, $1s3d$	1.5[a]	1.2	1.71 (1.88)[a]	0.54		0.86	0.77
$(2,1_5)$	$1s4s$, $1s4d$	0.48	0.39	0.53 (0.52)	0.53	0.32	0.45	0.76
$(2,1_6)$	$1s5s$, $1s5d$	0.38	0.34	0.51 (0.51)	0.51	1.0	0.47	0.77
$(2,1_7)$	$1s6s$, $1s6d$	0.36	0.34	0.49 (0.47)	0.49	1.16	—	0.75

[a]For the $(2,1_4)$ state, the strongest states are $1s3s$ and $1s3d$, but the branching ratio given is for transitions to the third and fourth strongest channels, $1s4s$ and $1s4d$, whose wavelengths are sufficiently close not to be influenced by the spectrometer transmission.

V. DISCUSSION

Our experimental data are in good overall agreement with the calculations where quantitative comparison can be carried out. There are some small discrepancies and we can invert the data to obtain the experimental branching ratios from the excited $^1P^o$ parent states to the main $^1S^e$ and $^1D^e$ intermediate states. This is presented in Table II. The procedure is simple and based on published calculated fluorescence decay rates [19] which, as stated above, are in good agreement with the *ab initio* calculations [17]. Taking the example of Fig. 5 the parent $^1P^o$ $(2,0_4)$ state decays mainly to $^1S^e$ $1s4s$ and $^1D^e$ $1s4d$ states and we have measured the $1s4s \rightarrow 1s2p$ and $1s4d \rightarrow 1s2p$ transition intensities. They are close together in wavelength and so the transmission of the spectrometer does not affect the results. We know [19] that the branching ratios of $1s4s$ and $1s4d$ states for fluorescent decay into the $1s2p$ state are $B_{2,1}=0.59$ and $B_{14,1}=0.74$, respectively, see Eq. (1). Thus the initial populations of the $1s4s$ and $1s4d$ states, and therefore the branching ratio from the parent $^1P^o(2,0_4)$ state ($i=13$), is estimated by

$$\left(\frac{\Gamma^r_{1s\ 4s,13}}{\Gamma^r_{1s\ 4d,13}}\right)_{exp} = Y\frac{0.74}{0.59}\frac{I(1s4s \rightarrow 1s2p)}{I(1s4d \rightarrow 1s2p)},$$

where I represents the measured intensity of a given fluorescence transition (1) and Y is the above-mentioned angular factor, equal for all $1snd \rightarrow 1s2p$ transitions in the second step of the cascade.

This approximation is expected to work very well because the branching ratio for $1snp$ decay to the ground state or to the metastable $1s2s$ state is more than 0.98 for $n=3-8$ [19]. Thus most of the observed line intensity comes from the second step of the three-step decay

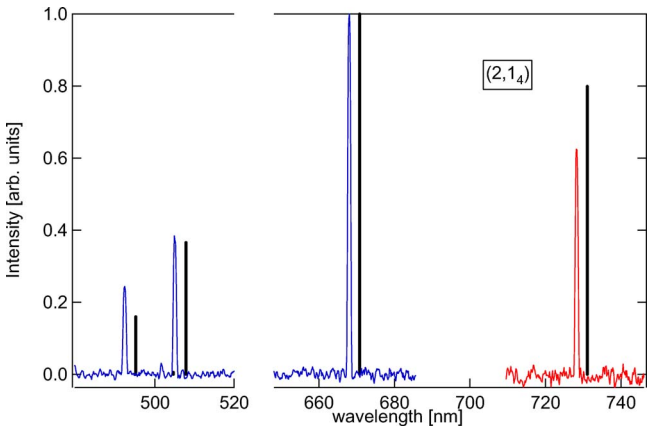

FIG. 6. (Color online) PIF spectrum of the $(2,1_4)$ state.

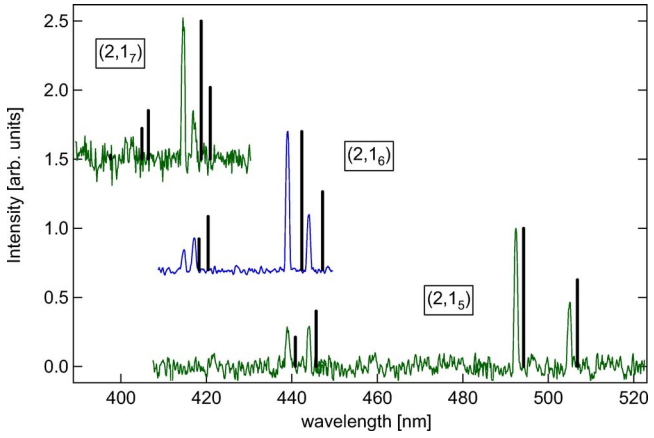

FIG. 7. (Color online) PIF spectrum for excitation to the $(2,1_n)$ states ($n=5-7$).

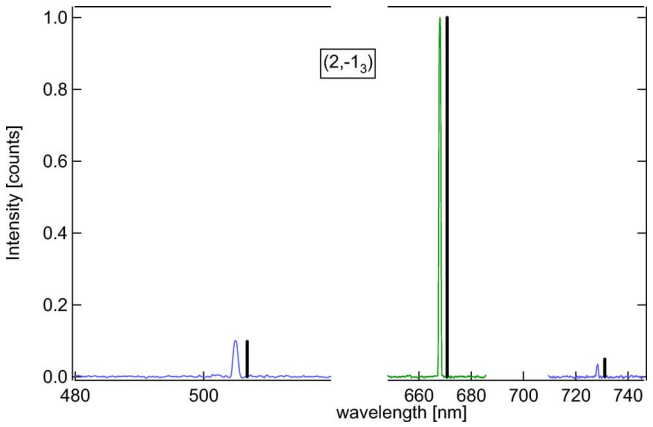

FIG. 8. (Color online) PIF spectrum for excitation to the $(2, -1_3)$ state.

$$^1\mathrm{P}^0 \rightarrow (^1\mathrm{S}^e, ^1\mathrm{D}^e) + h\nu(\mathrm{VUV}) \rightarrow {}^1\mathrm{P}^0 + h\nu(\mathrm{visible})$$
$$\rightarrow \text{ground state} + h\nu(\mathrm{VUV}),$$

since there is a very low probability of more complex cascades, that may populate the main lines in the final step of the decay ($^1\mathrm{P}^o \rightarrow {}^1\mathrm{S}^e \rightarrow {}^1\mathrm{P}^o \rightarrow {}^1\mathrm{S}^e$ or $^1\mathrm{P}^o \rightarrow {}^1\mathrm{D}^e \rightarrow {}^1\mathrm{P}^o \rightarrow {}^1\mathrm{S}^e$, etc). At higher values of n, these processes become more important for the low energy transitions, which are in any case weak, but they can be modeled quantitatively by the method described in Sec. III.

The present data can be compared, in part, with the results of Schartner *et al.* [12], as well as the very recent data of Mickat *et al.* [22] and in Table II we have included intensity ratios derived from their data. Qualitatively, our results agree with the conclusion that the $(2,-1_n)$ states decay almost exclusively to 1*snd* states, although we observed weak emission from other predicted lines. The quantitative agreement with the data of Schartner *et al.* for the other series of states is not good, with discrepancies in the ratios for the $(2,0_n)$ and $(2,1_n)$ lines of about a factor of 2 to 3, which may be due to their use of a different geometry (emission is anisotropic) or to the high pressure used in this pioneering study, 0.1 mbar. These authors detected emission perpendicular to the incident photon electric vector, but our calculations suggest that accounting for this factor would make the discrepancy between the data sets worse. In their geometry, the polarization of the emitted light has to be taken into account, so the ratios may depend on the transmission of the spectrometer. In our case, there is no polarization dependence as the detection is along the incident electric vector, and so the setup has cylindrical symmetry. On the other hand, our calculated asymmetry parameters were successfully employed to explain the measured angular distribution of VUV photons [20], which is further evidence of the reliability of our calculations.

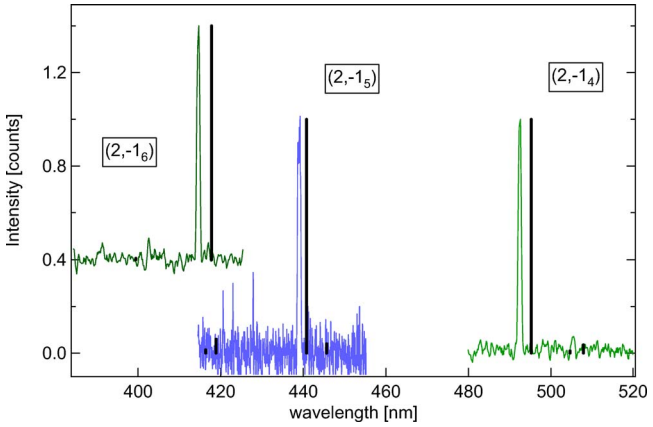

FIG. 9. (Color online) PIF spectrum for excitation to the $(2, -1_n)$ states ($n=4-6$).

The agreement with Mickat *et al.* [22] is better. For the $(2,0_n)$ series [denoted $(n,+1)$ in their notation], we obtain the same ratio for the first member and then our values are almost constant, while those of Mickat *et al.* increase. Both data sets show reasonable agreement with theory, but there are differences between the data, with our values being consistently below the theoretical prediction, and those of Mickat *et al.* too low for $n=4$, and too high for $n=7$. For the $(2,1_n)$ series [denoted $(n,-1)$ in their notation], the two data points for the ratio of the two strongest transitions and $n=5$ and 6 can be compared, and the data of Mickat *et al.* is closer to the theoretical values. For $n=4$ we can compare the ratio of the third to the fourth strongest transitions and our value (1.2) is about 30% below the theoretical value calculated with the velocity gauge, whereas the value of Mickat *et al.* is more than 40% lower. Our data set is slightly more comprehensive as we include the $n=7$ state.

Liu *et al.* [21] have calculated the relative branching ratio of fluorescence into 1*sns* and 1*snd* lines, using a complex rotation method and Rayleigh-Ritz variation with the *B*-spline functions for generation of doubly excited and singly excited states, respectively,

$$\Gamma^r_{s,i} = \sum_j \Gamma^r_{j,i}, \quad \Gamma^r_{d,i} = \sum_j \Gamma^r_{j,i}, \tag{3}$$

where $\Gamma^r_{s,i}$, $\Gamma^r_{d,i}$ are the total transition rates to 1*sns* or 1*snd* states, j runs over all 1*sns* or all 1*snd* states. Because the ratio of the two most intense 1*sns* and 1*snd* transitions practically coincide with the ratio of the two terms in Eq. (3) we have included the comparison with the data of Liu in Table II. We note that both theories [17] and [21] seem to overestimate transitions into 1*sns* states relative to 1*snd*. In the case of the $(2,0_n)$ resonances, Zitnik *et al.* [17] report values with a larger discrepancy with respect to the experimental values, while for $(2,1_n)$ Liu *et al.* [21] predict a higher ratio.

The study of Mickat *et al.* [22] was carried out with a different apparatus and different experimental difficulties were encountered: their pressure was at least an order of magnitude higher than ours, but against this they do not appear to have had difficulty with stability of the incident photon energy; they scanned the PIFS spectrometer wavelength whereas we used parallel acquisition; we corrected for anisotropy using calculated values of β, whereas they measured anisotropy, albeit with different angular acceptance in the two geometries used. In addition, in the present theory there are some small differences between the length and velocity gauges, and larger differences between the present and other

calculations. It is therefore difficult to know where the discrepancies between theory and experiment arise. However the overall agreement within 10 to 30 % appears quite reasonable.

VI. SUMMARY

The PIFS spectra of the lower states of the helium singlet doubly excited states have been measured, and compared with theory. Satisfactory agreement was obtained with theory, and we assume that the remaining differences originate from the most difficult and least tested part of the theory, treating the first VUV fluorescence decay of correlated doubly excited states. Taking the singly excited cascade branching ratios as known parameters the measured fluorescence intensities allow us to invert the data and estimate the branching ratios of the fluorescence decay from the parent doubly excited state, in the first step of the cascade.

ACKNOWLEDGMENTS

We thank A. Kivimäki for experimental assistance, and all our colleagues at Elettra, particularly Luca Romanzin for construction of the YAP detector and Mauro Trovò for technical assistance.

[1] P. G. Kruger, Phys. Rev. **36**, 855 (1930).
[2] R. P. Madden and K. Codling, Phys. Rev. Lett. **10**, 516 (1963); Astrophys. J. **141**, 364 (1965).
[3] M. Domke, K. Schulz, G. Remmers, G. Kaindl, and D. Wintgen, Phys. Rev. A **53**, 1424 (1996).
[4] M. K. Odling-Smee, E. Sokell, P. Hammond, and M. A. MacDonald, Phys. Rev. Lett. **84**, 2598 (2000).
[5] Jan-Erik Rubensson, Conny Såthe, Stefan Cramm, Barbara Kessler, Stefano Stranges, Robert Richter, Michele Alagia, and Marcello Coreno, Phys. Rev. Lett. **83**, 947 (1999).
[6] Thomas Ward Gorczyca, Jan-Erik Rubensson, Conny Såthe, Magnus Ström, Marcus Agåker, Dajun Ding, Stefano Stranges, Robert Richter, and Michele Alagia, Phys. Rev. Lett. **85**, 1202 (2000).
[7] K. C. Prince, R. Richter, M. de Simone, M. Alagia, and M. Coreno, Phys. Rev. A **68**, 044701 (2003).
[8] B. Krässig, E. P. Kanter, S. H. Southworth, R. Guillemin, O. Hemmers, D. W. Lindle, R. Wehlitz, and N. L. S. Martin, Phys. Rev. Lett. **88**, 203002 (2002).
[9] K. Schulz, G. Kaindl, M. Domke, J. D. Bozek, P. A. Heimann, A. S. Schlachter, and J. M. Rost, Phys. Rev. Lett. **77**, 3086 (1996).
[10] F. Penent, P. Lablanquie, R. I. Hall, M. Žitnik, K. Bucar, S. Stranges, R. Richter, M. Alagia, P. Hammond, and J. G. Lambourne, Phys. Rev. Lett. **86**, 2758 (2001).
[11] J. G. Lambourne, F. Penent, P. Lablanquie, R. I. Hall, M. Ahmad, M. Žitnik, K. Bučar, P. Hammond, S. Stranges, R. Richter, M. Alagia, and M. Coreno, J. Phys. B **36**, 4339 (2003).
[12] K.-H. Schartner, B. Zimmermann, S. Kammer, S. Mickat, H. Schmoranzer, A. Ehresmann, H. Liebel, R. Follath, and G. Reichardt, Phys. Rev. A **64**, 040501(R) (2001).
[13] K. C. Prince, R. R. Blyth, R. Delaunay, M. Zitnik, J. Krempasky, J. Slezak, R. Camilloni, L. Avaldi, M. Coreno, G. Stefani, C. Furlani, M. de Simone, and S. Stranges, J. Synchrotron Radiat. **5**, 565 (1998).
[14] M. Coreno, M. de Simone, M. Danailov, R. Richter, A. Kivimäki, M. Zitnik, and K. C. Prince, J. Electron Spectrosc. Relat. Phenom. **144–147**, 39 (2005).
[15] NIST database, http://webbook.nist.gov/chemistry/
[16] L. Lipsky, R. Anania, and M. J. Conneely, At. Data Nucl. Data Tables **20**, 127 (1977).
[17] M. Žitnik, K. Bucar, M. Štuhec, F. Penent, R. I. Hall, and P. Lablanquie, Phys. Rev. A **65**, 032520 (2002).
[18] C. Froese Fischer, T. Brage, and P. Jonsson, *Computational Atomic Structure* (Institute of Physics Publishing, London, 1997).
[19] C. E. Theodosiou, At. Data Nucl. Data Tables **36**, 97 (1987).
[20] J. G. Lambourne, F. Penent, P. Lablanquie, R. I. Hall, M. Ahmad, M. Žitnik, K. Bučar, P. Hammond, S. Stranges, R. Richter, M. Alagia, and M. Coreno, J. Phys. B **36**, 4351 (2003).
[21] Chien-Nan Liu, Ming-Keh Chen, and C. D. Lin, Phys. Rev. A **64**, 010501(R) (2001).
[22] S. Mickat, K.-H. Schartner, Sv. Kammer, R. Schill, L. Werner, S. Klumpp, A. Ehresmann, H. Schmoranzer, and V. L. Sukhorukov, J. Phys. B **38**, 2613 (2005).